Physica E 84 (2016) 146–151

Contents lists available at ScienceDirect

Physica E

journal homepage: www.elsevier.com/locate/physe

Computational study of edge configuration and the diameter effects on the electrical transport of graphdiyne nanotubes

Boshra Ghanbari Shohany, Mahmood Rezaee Roknabadi *, Ahmad Kompany

Department of Physics, Faculty of Science, Ferdowsi University of Mashhad, Mashhad, Iran

HIGHLIGHTS

- The structural and electronic properties of graphdiyne nanotubes studied via ab initio.
- .The effects of edge configuration and diameter on the electrical properties are determined.
- All the nanotubes exhibited semiconducting behavior with direct transition at Γ point.
- The zigzag nanotubes have smaller band gap and higher current comparing to the armchair.

GRAPHICAL ABSTRACT

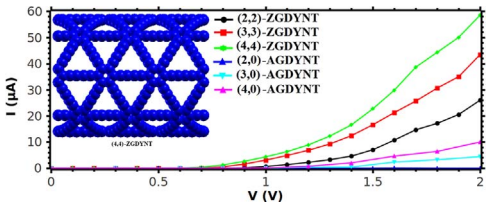

ARTICLE INFO

Article history:
Received 31 January 2016
Received in revised form
21 April 2016
Accepted 27 May 2016
Available online 27 May 2016

Keywords:
Computational study
Armchair graphdiyne nanotube
Zigzag graphdiyne nanotube
Electrical transport properties

ABSTRACT

In this work, the structural and electronic properties of armchair and zigzag graphdiyne nanotubes (GDYNTs) have been investigated using the density functional theory (DFT). All the nanotubes under investigation exhibited semiconducting behavior. The edge configuration and diameter effects on the electrical transport of graphdiyne nanotubes are studied using non-equilibrium Green's function (NEGF) method. Our results showed that the currents in the zigzag graphdiyne nanotubes are remarkably higher comparing to the armchair nanotubes.

1. Introduction

During the past two decades, organic materials have been recognized as promising candidates to be used in fabricating new generation of electronic and optoelectronic devices. Among these materials, carbon-rich molecules have attracted much more attentions for using in nanotechnology and the related area. However, the new carbon structures are still under consideration [1–15].

Graphdiyne (GDY) which was first predicted by Haley et al. in 1997 belongs to the graphyne family [16]. Graphdiyne possesses both sp and sp^2-hybridized carbon atoms. The sp^2-hybridized carbon atoms create hexagonal rings, and are linked by diacetylenic linkages which consist of sp-hybridized carbon atoms [17–20]. Graphdiyne is predicted to be the most stable among the various diacetylenic non-natural carbon allotropes which have been studied so far [21,22].

Graphdiyne nanotubes were developed for the first time during 2003–2004, by rolling graphdiyne sheets to make seamless cylinders [23]. Ten years later, Li et al. reported the preparation of graphdiyne nanotube arrays through association of a template technique and catalyzed cross-coupling reaction [24]. Their results showed that GDYNT arrays have excellent field emission properties. GDYNTs were synthesized by this method exhibiting a reduced value of work function and showed to be more stable than carbon nanotubes.

* Corresponding author.
E-mail address: roknabad@um.ac.ir (M.R. Roknabadi).

http://dx.doi.org/10.1016/j.physe.2016.05.040
1386-9477/

However, many properties of graphdiyne nanotubes are still remained unknown. To our knowledge, only recently, a single-layer sheet and (3, 3) nanotube of graphdiyne have been studied by Jalili et al., in 2015, theoretically [25]. Their results showed that the charge carrier mobility of the graphdiyne nanotube is higher than both graphdiyne sheet and the carbon nanotube.

In this work, first-principle calculations were employed to investigate the structural and electronic properties of armchair and zigzag graphdiyne nanotubes having different diameters. The effects of edge configuration and diameter on their electrical transport properties are also determined, which up to our knowledge have not already been studied.

2. Computational method

A single-walled carbon nanotube (CNT) is formed by rolling a graphene sheet to make a seamless cylinder. In the same way, GDYNT can be formed by rolling a graphdiyne sheet. As shown in Fig. 1, the nomenclature (n, m) can also be employed for GDYNTs, which (n, n) and (n, 0) represent zigzag and armchair GDYNTs, respectively [26]. These two types of graphdiyne nanotubes, with different diameters, are studied in the present work. The diameter of graphdiyne nanotube is given by $d=\frac{a}{\pi}\sqrt{n^2+nm+m^2}$, where a is the lattice constant of the graphdiyne sheet [27]. The following steps were performed to obtain the nanotube's coordinates:

1. Coordinates of the zigzag unit cell (x, y), which is shown by red lines in Fig. 1, were calculated manually. The results are given in Table 1. The coordinates of the armchair unit cell were obtained by the exchange of x and y.
2. By using the following formula, the unit cell of the sheet was converted to a cylinder:

$$x' = r\ \cos\left(\frac{x}{r}\right) y' = r\ \sin\left(\frac{x}{r}\right) z' = y \tag{1}$$

where r is the radius of the tube.

3. The other coordinates were obtained using

$$x' = r\ \cos\left(\theta' + \frac{x}{r}\right) y' = r\ \sin\left(\theta' + \frac{x}{r}\right) z' = y \tag{2}$$

where $\theta' = 2\pi/n$.

The geometry relaxation and electronic structure calculations

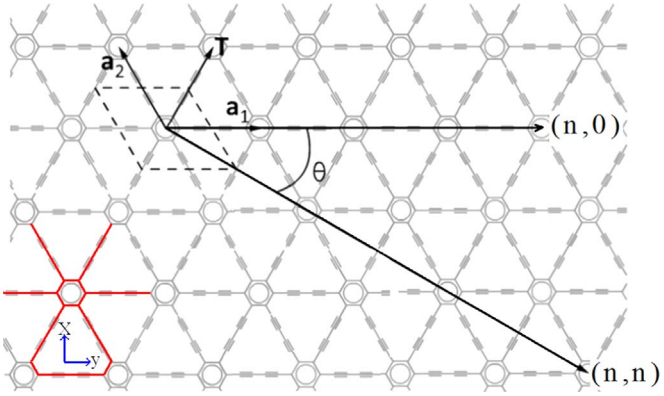

Fig. 1. Chiral and transition vectors for zigzag and armchair graphdiyne nanotubes. The rhombus drawn with dashed lines represents the unit cell. The unit cell of zigzag graphdiyne nanotube was shown by red lines at the bottom left. (For interpretation of the references to color in this figure legend, the reader is referred to the web version of this article.)

Table 1.
Coordinates of the unit cell of zigzag Graphdiyne nanotubes.

	x	y
1	0.7	1.415
2	0.7	2.815
3	0.7	4.045
4	0.7	5.375
5	0.7	6.605
6	0.7	8.005
7	1.938	0.7
8	3.15	1.4
9	4.216	2.015
10	5.367	2.68
11	6.433	3.295
12	7.646	3.995
13	7.646	5.425
14	6.433	6.125
15	5.367	6.74
16	4.216	7.405
17	3.15	8.02
18	1.938	8.72
19	15.82905	0.7
20	14.621	1.4
21	13.555	2.015
22	12.404	2.68
23	11.338	3.295
24	10.126	3.995
25	10.126	5.425
26	11.338	6.125
27	12.404	6.74
28	13.555	7.405
29	14.621	8.02
30	15.82905	8.72
31	8.884	0.745
32	8.884	1.975
33	8.884	3.375
34	8.884	6.045
35	8.884	7.445
36	8.884	8.675

were performed using linear combination of atomic orbitals (LCAO) as implemented in the SIESTA package [28]. The exchange-correlation functional of the electrons was described by the generalized gradient approximation (GGA) of Perdew-Burke-Ernzerhof (PBE). A double-zeta polarized basis set (DZP) was adopted for all structures. An energy cutoff of 200 Ry was chosen and the vacuum layers were set 10 Angstrom in the non-periodic directions to prevent the interaction of adjacent tubes. The Brillouin zone k-point sampling was $1 \times 1 \times 5$ for all the nanotubes, based on the Monkhorst-Pack method. The nanotubes were relaxed until the residual forces on each atom were reached below 0.01 eV/Å. The temperature was set as 300 K for all calculations.

The transport properties of graphdiyne nanotubes were computed using standard DFT calculations combined with non-equilibrium Green's functional techniques, which were carried out in the TranMain code of OpenMX package [29]. For the NEGF formalism, the system was divided in three parts: the left electrode (L), the scattering region (CC) and the right electrode (R). It was assumed that the electrodes were coupled only with the scattering region, but not with each other. Conduction in 1D system could be viewed as a transmission problem. The electric current through the scattering region at a finite bias voltage (V) was evaluated using the Landauer -Buttiker formula:

$$I(V) = \frac{2e^2}{h} \int_{-\infty}^{+\infty} \left\{ T(E, V)\left[f\left(E,\mu_L\right) - f\left(E,\mu_R\right)\right]\right\} dE \tag{3}$$

where e is the electron charge, h is Planck's constant, f is the Fermi

distribution function at a certain temperature (T), $\mu_{L/R}$ are the chemical potentials of the left/right electrod]es with $\mu_{L/R}=E_F \pm eV/2$ shifted up and down relative to the Fermi energy and T (E, V) is the transmission probability at energy E and voltage $V=(\mu_L-\mu_R)/e$, that is given by

$$T(E, V)=Tr[\Gamma_L(E, V)G_{CC}(E, V)\Gamma_R(E, V)G^{+}_{CC}(E, V)] \quad (4)$$

where, $\Gamma_{L/R}$ is the coupling matrix between the scattering region and left/right electrode and G_{CC} (G^{+}_{CC}) is the retarded (advanced) Green's function of the scattering region:

$$\Gamma_{L/R} = i\left(\Sigma_{L/R} - \Sigma^{+}_{L/R}\right) \quad (5)$$

$$G_{CC} = \left[ES_{CC} - \left(\sum_L + \sum_R + H_{CC}\right)\right]^{-1} \quad (6)$$

S_{CC}, H_{CC} and $\sum_{L/R}$ are the overlap matrice, Hamiltonian and self-energy of the left/right electrodes, respectively. The self-energies contain the information regarding the available states in the electrodes at a given energy. Electrons can propagate from the scattering region into these available states. The self-energy can be written as [30–35]:

$$\Sigma_{L/R}=(ES_{L/RC} - H_{L/RC})G_{LL/RR}(ES_{CL/R} - H_{CL/R}) \quad (7)$$

$$G_{LL/RR} = (ES_{LL/RR} - H_{LL/RR})^{-1} \quad (8)$$

3. Results and discussion

3.1. Structural properties

The geometry optimization of the structures was carried out using SIESTA package. Fig. 2 represents three-dimensional view of (a) armchair and (b) zigzag graphdiyne nanotubes, after relaxation. The optimized bond lengths of the nanotubes are given in Table 2. The obtained values for graphdiyne nanotubes are equal to that of the graphdiyne sheet and the nanoribbons [36]. C–C bond lengths in the hexagon rings and diacetylenic linkages are different, implying that C–C hybridization in C links of graphdiyne nanotubes are not equal. This difference leads to the greater structural flexibility of GDYNTs in comparison with graphene [37]. As it can be seen in Fig. 2, the important difference between GDYNTs and CNTs is that the graphdiyne nanotubes have uniformly distributed pores on their sidewalls. This is an important characteristic, because these pores could simplify the electron transport through the nanotube sidewalls which may be significant for some applications such as hydrogen storage.

3.2. Electronic properties

Ab initio density functional calculations have been performed using the SIESTA code for evaluating the band structure of the nanotubes. The energy band gap of the zigzag and armchair graphdiyne nanotubes are plotted in Figs. 3 and 4, respectively. Fermi level is chosen at zero point. All the nanotubes show semiconducting behavior with direct transition at Γ point in the first Brillouin zone. The value of the band gaps and the diameters of these structures are presented in Table 3. As it can be seen, due to the quantum confinement effect, the band gaps of both zigzag and armchair graphdiyne nanotubes are clearly diameter dependent which decrease by increasing the diameter of the nanotube. In addition, AGDYNTs have larger band gap and smaller diameter in comparison with ZGDYNTs.

Figs. 5 and 6 show the density of states (DOS) of the zigzag and armchair graphdiyne nanotubes, respectively. The density of states at the Fermi level is zero, confirming the semiconducting behavior of the graphdiyne nanotubes. As observed in these figures, by increasing the diameter of the nanotubes the energy band gap decreases and the density of states increases.

In order to gain a deep insight into the electronic structure of

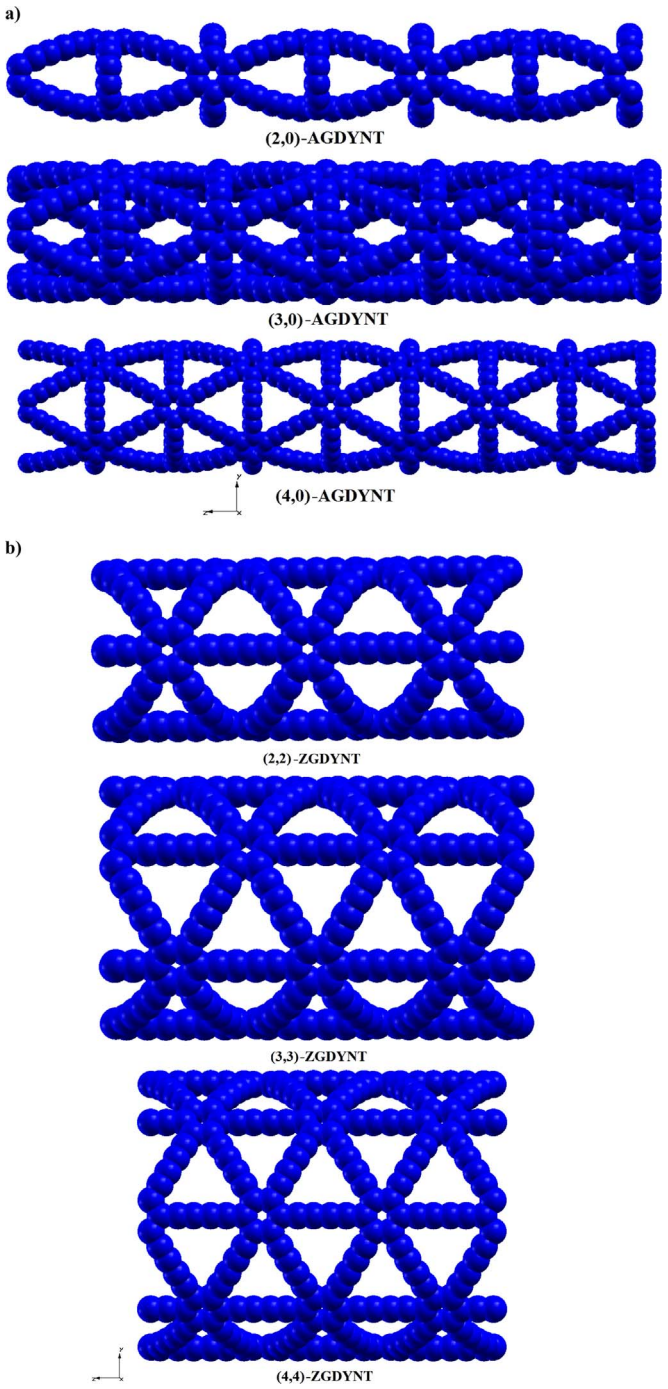

Fig. 2. Three-dimensional view of the (a) armchair and (b) zigzag graphdiyne nanotubes after relaxation.

Table 2.
The optimized bond lengths of graphdiyne nanotubes.

Bonds type	Optimized length (Å)
=C = C=	1.43
=C – C≡	1.40
–C ≡ C –	1.24
≡C – C≡	1.35

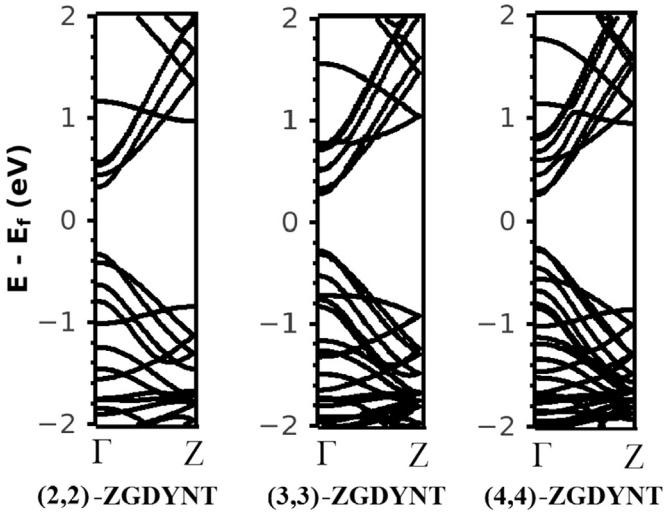

Fig. 3. The energy band gap of zigzag graphdiyne nanotubes.

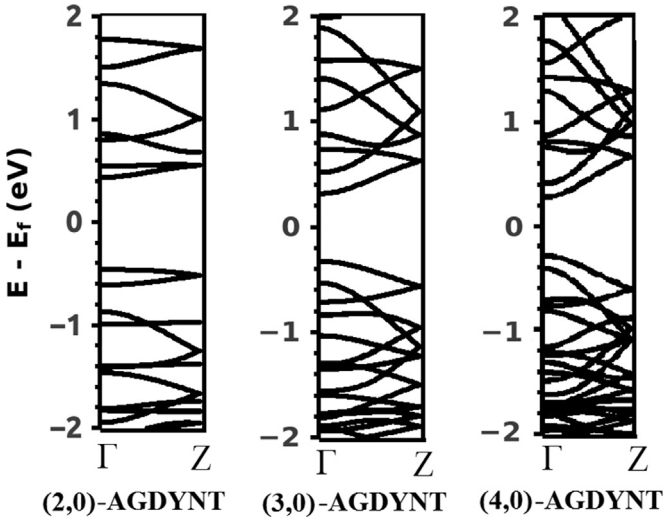

Fig. 4. The energy band gap of armchair graphdiyne nanotubes.

Table 3.
The values of energy gap and diameter of graphdiyne nanotubes.

Structure	Energy gap (eV)	Diameter (Å)
(2,2)-ZGDYNT	0.65	10.25
(3,3)-ZGDYNT	0.55	15.56
(4,4)-ZGDYNT	0.50	20.81
(2,0)-AGDYNT	0.95	6.42
(3,0)-AGDYNT	0.65	9.08
(4,0)-AGDYNT	0.55	12.04

graphdiyne nanotubes, the total, local and partial density of states of (4, 4) zigzag graphdiyne nanotube were calculated, as shown in Fig. 7. It was found that 2s and $2P_y$ orbitals have almost similar spectrum with zero value around the Fermi energy, while the $2p_x$ and $2p_z$ orbitals display the same wave shapes. From the PDOS and LDOS spectra, it can be seen that C–C hybridization in hexagon rings and diacetylenic linkages of graphdiyne nanotubes are different, which is in good agreement with the structural results.

3.3. Transport properties

To study the transport behavior of graphdiyne nanotubes, the current versus bias voltage (I-V) curve was computed using the

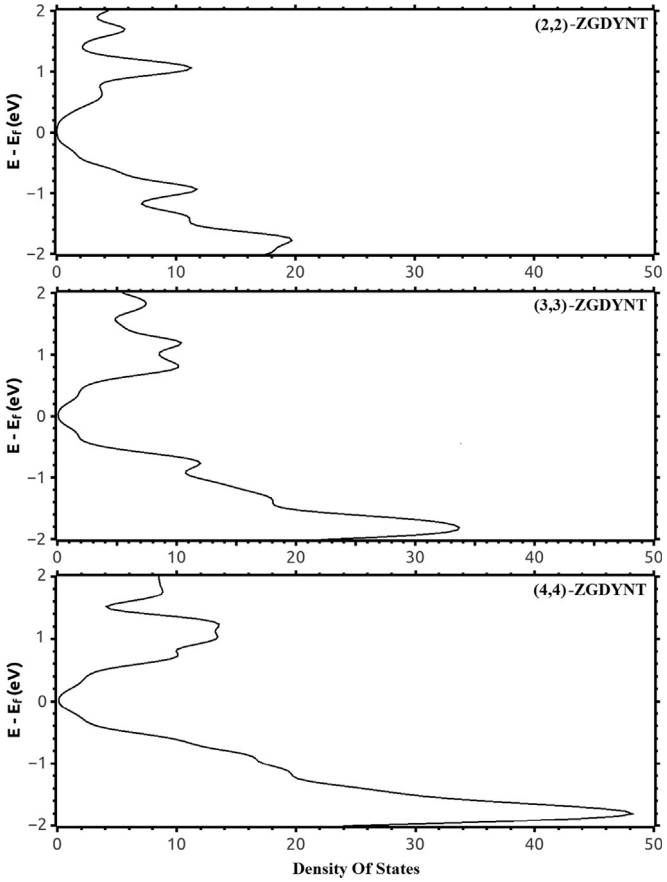

Fig. 5. The density of states (DOS) of the zigzag graphdiyne nanotubes.

two probe system. The scattering region is seamlessly connected to the two semi-infinite electrodes with the same structures. Fig. 8 shows the *I–V* characteristic of all configurations at the bias voltage in the range of 0.0–2.0 V. For all these nanotubes, the current becomes remarkable when the bias voltage exceeds the band gap value. As shown in Fig. 9, a threshold voltage equal to 0.6 V can be seen in the 4-ZGDYNT which has the band gap value $=0.5$ eV. Below this voltage, the current is almost zero and increases above this voltage. By increasing the diameter of the nanotubes, the band gap value of the nanotubes decreases and their density of states increases. In other words, electrons need less energy to transit from the valence band to the conduction band causing the current increases. Furthermore, the current in the zigzag nanotubes are higher than that of the armchairs.

The negative differential resistance (NDR) behavior is evident in (2, 0) armchair graphdiyne nanotube, as shown in Fig. 8. The peak-valley ratio (PVR), which is defined as the ratio of the peak current to the valley current, is often used to describe NDR behavior [38]. The calculated PVR value for (2, 0) armchair graphdiyne nanotube was obtained to be 43.08. To understand the NDR mechanism, the transmission spectra of (2, 0) armchair graphdiyne nanotube at the bias voltage of 1.4, 1.6 and 1.8 V are presented in Fig. 10. Bias windows $[-eV/2, +eV/2]$ are specified by red dashed lines. By increasing the bias voltage from 1.4 to 1.6 V, the transmission coefficient increases in the bias window. So that the current, which is determined by integrating the transmission function in the bias window, also increases. Then in the voltage range of 1.6–1.8 V, the transmission coefficient decreases in the bias window. As a result, the current decreases dramatically, showing NDR behavior at 1.6 V. This behavior can be explained by coupling change between the scattering region orbitals and the incident states in the electrodes under various biases [39,40]. The

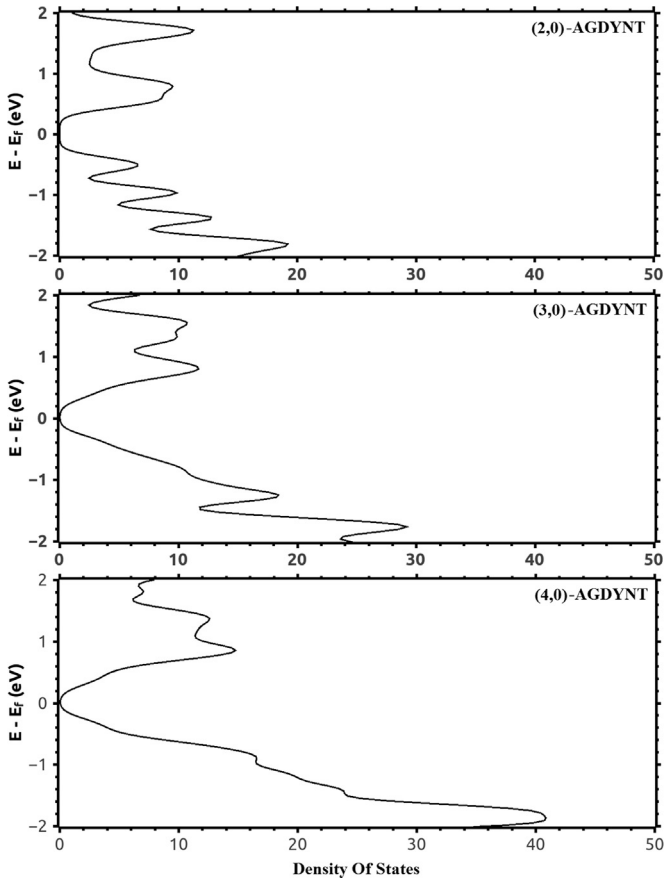

Fig. 6. The density of states (DOS) of the armchair graphdiyne nanotubes.

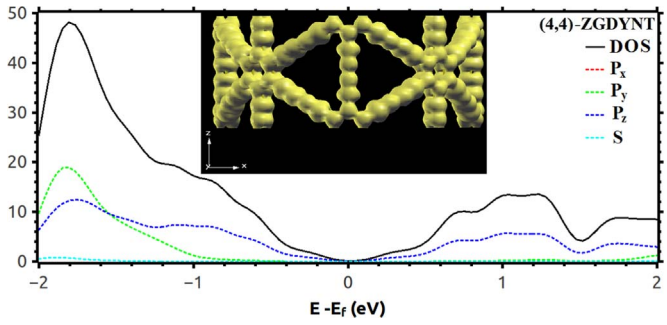

Fig. 7. The total, local and partial density of states of (4, 4) zigzag graphdiyne nanotube.

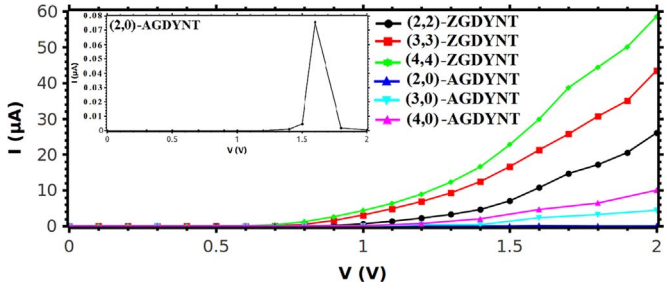

Fig. 8. *I–V* curves of graphdiyne nanotubes in the bias voltage in the range of 0.0–2.0 V.

negative differential resistance effect has been observed in some similar structures such as zigzag graphene nanoribbon [41], 6, 6, 12 graphyne nanoribbon [42,43], zigzag α-graphyne nanoribbon [44], armchair α-graphyne nanoribbon (PVR=1.4) [45] and carbon

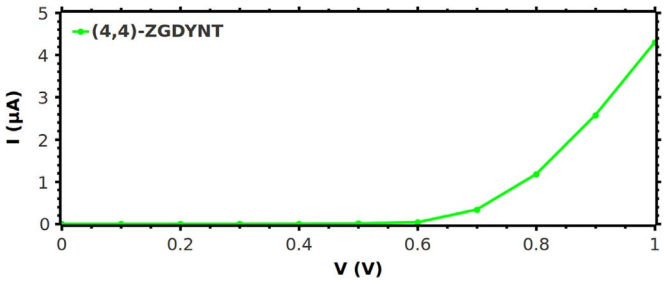

Fig. 9. *I–V* curve of 4-zigzag graphdiyne nanotube in the bias voltage in the range of 0.0–1.0 V.

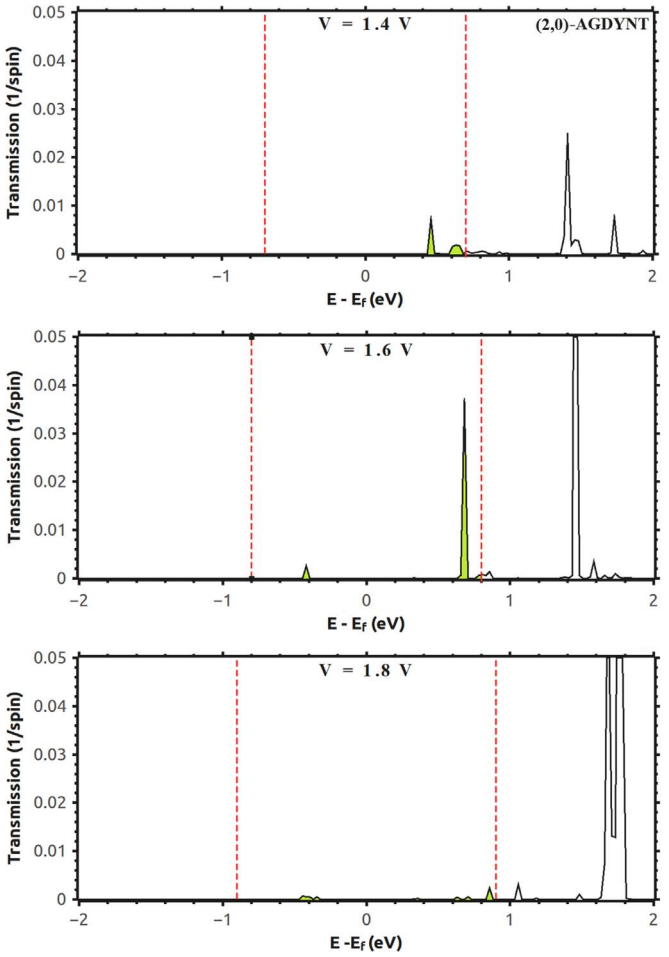

Fig. 10. The transmission spectra of (2, 0) armchair graphdiyne nanotube at bias voltages of 1.4, 1.6 and 1.8 V.

boronitride heteronanotubes (PVR=2–4) [46].

4. Conclusion

The structural, electronic and electrical properties of graphdiyne nanotubes were investigated using DFT and NEGF methods. It was found that C–C bond lengths are not equal, which results in the different C–C hybridization in hexagon rings and diacetylenic linkages. Since, the graphdiyne nanotubes have uniformly distributed pores sidewalls, so it seems to be interesting for some applications such as hydrogen storage. All the investigated nanotubes exhibited semiconducting behavior with direct transition at the Γ point. Our results showed that the energy band gap width is sensitive to the nanotubes diameter. The energy gap was found to

be inversely proportional to the diameter of the graphdiyne nanotubes, due to the quantum size effect. By increasing the diameter of GDYNTs, the band gap decreases while the current increases. Also, it was shown that the zigzag nanotubes have smaller energy band gap and higher current comparing to the armchair nanotubes. The NDR behavior was observed in (2, 0) armchair graphdiyne nanotube with the PVR equal to 43.08 at the bias voltage in the range of 1.4–1.8 V.

Acknowledgment

The authors gratefully acknowledge the Sheikh Bahaei National High Performance Computing Center (SBNHPCC) for providing computing facilities and time. SBNHPCC is supported by Scientific and Technological Department of Presidential Office and Isfahan University of Technology (IUT), Iran.

References

[1] V.R. Coluci, S.F. Braga, S.B. Legoas, D.S. Galvao, R.H. Baughman, J. Nanotechnol. 15 (2004) 142.
[2] V.R. Coluci, S.F. Braga, S.B. Legoas, D.S. Galvao, R.H. Baughman, J. Phys. Rev. B 68 (2003) 35430.
[3] Y. Jing, G. Wu, L. Guo, Y. Sun, J. Shen, Comput. Mater. Sci. 78 (2013) 22.
[4] K.S. Swapan, K. Ghosh, J. Phys. Chem. C 116 (2012) 5951.
[5] A.L. Ivanovskii, Prog. Solid State Chem. 41 (2013) 1.
[6] Y. Li, L. Xu, H. Liu, Y. Li, Chem. Soc. Rev. 43 (2014) 2572.
[7] N. Narita, S. Nagai, S. Suzuki, K. Nakao, Phys. Rev. B 58 (1998) 11009.
[8] U.H.F. Bunz, Y. Rubin, Y. Tobe, Chem. Soc. Rev. 28 (1999) 107.
[9] Q. Peng, A.K. Dearden, J. Crean, L. Han, S. Liu, X. Wen, S. De, Nanotechnol. Sci. Appl. 7 (2014) 1.
[10] G. Luo, X. Qian, H. Liu, R. Qin, J. Zhou, L. Li, Z. Gao, E. Wang, W.N. Mei, J. Lu, Y. Li, S. Nagase, Phys. Rev. B 84 (2011) 075439.
[11] M. Long, L. Tang, D. Wang, Y. Li, Z. Shuai, ACS Nano 5 (2011) 2593.
[12] J.M. Kehoe, J.H. Kiley, J.J. English, C.A. Johnson, R.C. Petersen, M.M. Haley, Org. Lett. 2 (2000) 969.
[13] J. Drogar, M.R. Roknabadi, M. Behdani, M. Modarresi, A. Kari, Superlattices Microstruct. 75 (2014) 340.
[14] J. Kang, J. Li, F. Wu, S.S. Li, J.B. Xia, J. Phys. Chem. C 115 (2011) 20466.
[15] T. Ouyang, Y. Chen, L.M. Liu, Y. Xie, X. Wei, J. Zhong, Phys. Rev. B 85 (2012) 235436.
[16] M.M. Haley, S.C. Brand, J.J. Pak, Angew. Chem. Int. Ed. Engl. 36 (1997) 836.
[17] H. Zhang, M. Zhao, X.H. Zhenhai, W. Xuejuan, Z.X. Liu, J. Phys. Chem. C 115 (2011) 8845.
[18] H. Zhang, X. He, M. Zhao, M. Zhang, L. Zhao, X. Feng, Y. Luo, J. Phys. Chem. C 116 (2012) 16634.
[19] C. Sun, D.J. Searles, J. Phys. Chem. C 116 (2012) 26222.
[20] H. Zhang, Y. Xia, H. Bu, X. Wang, M. Zhang, Y. Luo, M. Zhao, J. Appl. Phys. 113 (2013) 044309.
[21] G. Li, Y. Li, H. Liu, Y. Guo, Y. Li, D. Zhu, Chem. Commun. 46 (2010) 3256.
[22] H. Bu, M. Zhao, H. Zhang, X. Wang, Y. Xi, Z. Wang, J. Phys. Chem. A 116 (2012) 3934.
[23] V.R. Coluci, D.S. Galvao, R.H. Baughman, J. Chem. Phys. 121 (2004) 3228.
[24] G. Li, Y. Li, X. Qian, H. Liu, H. Lin, N. Chen, Y. Li, J. Phys. Chem. C 115 (2011) 2611.
[25] S. Jalili, F. Houshmand, J. Schofield, Appl. Phys. A 119 (2015) 571.
[26] X.M. Wang, S.S. Lu, J. Phys. Chem. C 117 (2013) 19740.
[27] L.C. Qin, Phys. Chem. Chem. Phys. 9 (2007) 31.
[28] J.M. Soler, E. Artacho, J.D. Gale, A. García, J. Junquera, P. Ordejón, D. Sánchez-Portal, J. Phys. Condens. Matter 14 (2002) 2745.
[29] T. Ozaki, Phys. Rev. B 59 (1999) 16061.
[30] J.E. Padilha, R.B. Pontes, A.J.R.D. Silva, A. Fazzio, Int. J. Quant. Chem. 111 (2011) 1379.
[31] J. Huang, W. Wang, S. Yang, H. Su, Q. Li, J. Yang, Chem. Phys. Lett. 539 (2012) 102.
[32] Y. Meir, N.S. Wingreen, Phys. Rev. Lett. 68 (1992) 2512.
[33] A.T. Johnson, L.P. Kouwenhoven, W.D. Jong, N.C. van der Vaart, C.J.P. M. Harmans, C.T. Foxon, Phys. Rev. Lett. 69 (1992) 1592.
[34] S. Ryu, C. Mudry, A. Furusaki, A.W.W. Ludwig, Phys. Rev. B 75 (2007) 205344.
[35] H. Ness, L.K. Dash, R.W. Godby, Phys. Rev. B 82 (2010) 085426.
[36] B.G. Shohany, M.R. Roknabadi, A. Kompany, Commun. Theor. Phys. 65 (2016) 99.
[37] A.L. Ivanovskii, Prog. Solid State Chem. 41 (2013) 1.
[38] J. Chen, M.A. Reed, A.M. Rawlett, J.M. Tour, Science 286 (1999) 1550.
[39] Z. Sohbatzadeh, M.R. Roknabadi, N. Shahtahmasebi, M. Behdani, Physica E 65 (2015) 61.
[40] L. Chen, Z. Hu, A. Zhao, B. Wang, Y. Luo, J. Yang, J.G. Hou, Phys. Rev. Lett. 99 (2007) 146803.
[41] J. Kang, F. Wu, J. Li, Appl. Phys. Lett. 98 (2011) 083109.
[42] Y. Ni, K.L. Yao, H.H. Fu, G.Y. Gao, S.C. Zhu, B. Luo, S.L. Wang, R.X. Li, Nanoscale 5 (2013) 4468.
[43] Y.H. Zhou, J. Zeng, K.Q. Chen, Carbon 76 (2014) 175.
[44] D. Zhang, M. Long, X. Zhang, J. Ouyang, H. Xu, K.S. Chan, RSC Adv. 6 (2016) 15008.
[45] W. Wu, GuoW, X.C. Zeng, Nanoscale 5 (2013) 9264.
[46] Y. Wu, P. Cheng, H. Zhu, Y. Huang, K. Zhang, R. Liao, Carbon 95 (2015) 220.